

Galactic evolution of rapid neutron capture process abundances: the inhomogeneous approach

B. Wehmeyer,¹ * M. Pignatari^{1,2} and F.-K. Thielemann¹

¹ *Univ Basel, Dept. Phys., Klingelbergstr. 82, CH-4056 Basel, Switzerland*

² *Konkoly Observatory, Research Centre for Astronomy and Earth Sciences, Hungarian Academy of Sciences, Konkoly Thege Miklós út 15-17, H-1121 Budapest, Hungary*

Unreferreed and unedited version as per June 16, 2015 (1); In original form January 30, 2015

ABSTRACT

For the origin of heavy r-process elements, different sources have been proposed, e.g., core-collapse supernovae or neutron star mergers. Old metal-poor stars carry the signature of the astrophysical source(s). Among the elements dominantly made by the r-process, europium (Eu) is relatively easy to observe. In this work we simulate the evolution of europium in our galaxy with the inhomogeneous chemical evolution model ‘ICE’, and compare our results with spectroscopic observations. We test the most important parameters affecting the chemical evolution of Eu: (a) for neutron star mergers the coalescence time scale of the merger (t_{coal}) and the probability to experience a neutron star merger event after two supernova explosions occurred and formed a double neutron star system (P_{NSM}) and (b) for the sub-class of magneto-rotationally driven supernovae (“Jet-SNe”), their occurrence rate compared to standard supernovae ($P_{\text{Jet-SN}}$). We find that the observed [Eu/Fe] pattern in the galaxy can be reproduced by a combination of neutron star mergers and magneto-rotationally driven supernovae as r-process sources. While neutron star mergers alone seem to set in at too high metallicities, Jet-SNe provide a cure for this deficiency at low metallicities. Furthermore, we confirm that local inhomogeneities can explain the observed large spread in the europium abundances at low metallicities. We also predict the evolution of [O/Fe] to test whether the spread in α -elements for inhomogeneous models agrees with observations and whether this provides constraints on supernova explosion models and their nucleosynthesis.

Key words: Galaxy: abundances – Galaxy: evolution – nuclear reactions, nucleosynthesis, abundances

1 INTRODUCTION

The rapid neutron capture process (r-process, e.g., Thielemann et al. 2011, and references therein) is responsible for the production of about half of the heavy element abundances beyond Fe in the solar system, and of the heaviest elements like Th and U. The remaining heavy element abundances are mostly made by the slow neutron capture process (s-process, e.g., Käppeler et al. 2011). Despite its relevance, the true astrophysical origin of the r-process is still under debate. Because of the larger uncertainties affecting the r-process nucleosynthesis predictions compared to the s-process in stars, the r-process isotopic contribution in the solar system has been originally identified by using the residual method, i.e., by subtracting the s-process component from the solar isotopic distribu-

tion (e.g., Arlandini et al. 1999, Bisterzo et al. 2014). The r-process residual abundances have been shown to be consistent in first approximation with the abundance signatures in old r-process rich metal-poor stars (at least for elements heavier than Ba, see Travaglio et al. 2004 for details), carrying the signature of the r-process nucleosynthesis in the early galaxy (e.g., Sneden, Cowan & Gallino 2008). For instance, Eu receives only a marginal contribution from the s-process (the s-process explains only 6 per cent of the solar Eu, while the remaining amount has an r-process origin, Bisterzo et al. 2014), and therefore it is often used as a tracer of the r-process nucleosynthesis in stellar spectroscopic observations. One possibility to test predictions from r-process nucleosynthesis is to include the r-process stellar yields in galactic chemical evolution (GCE) simulations, and to compare the theoretical results with spectroscopic observations at different metallicities. Eu is an ideal diagnostic for these studies. The purpose of this work is to illustrate the eu-

* benjamin.wehmeyer@unibas.ch

europium evolution throughout the evolution of our galaxy. We consider here the contribution from two sites (and their frequency) to the production of heavy r-process elements: Neutron Star Merger (NSM) and "magneto-rotationally driven supernovae" (hereafter referred to as "Jet-SNe"). We will show that the combination of both sites is able to reproduce the observed europium abundance distribution of the stars of our galaxy.

Neutron star - black hole (NS-BH) mergers might have a non-negligible contribution to the r-process inventory in the galaxy. However, their relevance as astrophysical source for the r-process is controversial, since this event has not yet been observed (e.g., Bauswein et al. 2014). These difficulties also result in an extreme divergence of the predicted galactic rate of such an event (e.g., Postnov & Yungelson 2014). However, it should be noticed that a contribution from NS-BH mergers has been predicted as well (e.g., Korobkin et al. 2012, Mennekens & Vanbeveren 2014). We give an estimate of the possible effects caused by these events in Section 5.

Chemical evolution of galaxies has made strong advances since its early days. Initially all approaches made use of the instantaneous recycling approximation in the sense, that the ejecta of stellar end stages were immediately utilized without delay after the initial star formation, assuming that the stellar evolution time scale is short in comparison to galactic evolution. If, in addition, the instantaneous mixing approximation was applied, i.e., assuming that the ejecta were instantaneously mixed throughout the galaxy, the whole galaxy acts as a homogeneous box. Neglecting this can explain radial gradients. Further developments included infall of primordial matter into and outflow of enriched material out of the galaxy (for a review of these early investigations see e.g., Audouze & Tinsley 1976). When relaxing the instantaneous recycling approximation, i.e., taking into account that (explosive) stellar ejecta enter the interstellar Medium (ISM) delayed with respect to the birth of a star by the duration of its stellar evolution, detailed predictions for the evolution of element abundances can be made. Based on nucleosynthesis predictions for stellar deaths, a number of detailed analyses have been performed, from light elements up to the Fe-group (e.g., Timmes et al. 1995, Goswami & Prantzos 2000, Matteucci 2001, Gibson et al. 2003, Kobayashi et al. 2006, Pagel 2009, Kobayashi 2012, Matteucci 2012). Such approaches have recently also been applied to understand the enrichment of heavy elements in the galaxy (including r-process contributions) as a function of time or metallicity [Fe/H] (see e.g., Ishimaru & Wanaajo 1999, Travaglio et al. 1999, De Donder & Vanbeveren 2003, Matteucci 2012, Vangioni et al. 2015).

However, if still the instantaneous mixing approximation is applied, i.e., such ejecta are instantaneously mixed with the global ISM, no local inhomogeneities can be produced. The latter would relate to the fact that only limited amounts of the ISM are polluted by / mixed with the ejecta of each event. This effect is of essential importance, especially at low metallicities, where portions of the ISM are already polluted by stellar winds and supernovae, and others are not. In addition, different portions of the ISM are polluted by different types of events, leading to a scatter at the same metallicity, which can in fact be utilized as a constraint for these different stellar ejecta. When, however, utilizing the instantaneous mixing approximation, this leads to

a unique relation between galactic evolution time and metallicity [Fe/H], i.e., any [Fe/H] can be related to a specific time in the evolution of a galaxy (while inhomogeneous mixing could experience similar [Fe/H] values in different locations of the galaxy at different times). This is especially the case in the very early galactic evolution ($[\text{Fe}/\text{H}] < -2.5$), when locally only a few stars (out of a whole initial mass function IMF) might have exploded and imprinted their stellar neighbourhood with their ejecta. Thus, the application of chemical evolution models which utilize the instantaneous mixing approximation is questionable for the early evolution of galaxies.

In addition, for each [Fe/H], due to the instantaneous mixing, only a mean value of $[X/\text{Fe}]$ (X being the element of interest to follow in chemical evolution) is obtained. Inhomogeneous mixing, however, could produce larger ratios in strongly polluted areas and smaller values in still less polluted ones. This means that the scatter in $[X/\text{Fe}]$ at low metallicities, which might also be a helpful asset in pointing to the origin of element X, cannot be reproduced or utilized with an homogeneous treatment. In case of rare events, which – on the other hand – produce large amounts of element X in each event, this would produce a large scatter, and – if observed – could be used as a very helpful constraint to identify the production site. For these reasons, specially for the origin of r-process elements like Eu, we think that only inhomogeneous chemical evolution models should be utilized at low metallicities. The two type of rare events (i) Jet-SNe (maybe up to 1% of all core collapse supernovae (CCSNe)) and (ii) neutron star mergers, with a similar occurrence frequency of about 1% of all CCSNe are considered here, while regular and more frequent core collapse supernovae might at most contribute to the lighter r-process elements. The binary merger rates are estimated by van den Heuvel & Lorimer (1996) as well as Kalogera et al. (2004). The rate of Jet-SNe is related to the fact that about 1% of neutron stars are found with magnetic fields of the order 10^{15} Gauss (magnetars, see, e.g., Kouveliotou et al. 1998, Kramer et al. 2009).

Earlier inhomogeneous chem(odynam)ical evolution models for r-process elements like Eu have been provided by Travaglio et al. (2001, where the r-process yields were assumed to come from CCSN), Argast et al. (2004) and Matteucci et al. (2014) comparing neutron star mergers and core collapse supernovae, Cescutti & Chiappini (2014, comparing NSM and Jet-SNe) Mennekens & Vanbeveren (with NSM and NS-BH mergers), and Shen et al. and van de Voort et al. (2015, only utilizing neutron star mergers). One of the main questions here is related to the problem of reproducing $[\text{Eu}/\text{Fe}]$ at low(est) metallicities. Cescutti & Chiappini (2014) have shown that this is possible with Jet-SNe. Argast et al. (2004) concluded that neutron star mergers cannot reproduce observations at $[\text{Fe}/\text{H}] < -2.5$, while van de Voort et al. (2015) and Shen et al. 2015 came to the opposite conclusion.

The main difference between Jet-SNe and neutron star mergers is that in one case the immediate progenitors are massive stars and the first occurrence in chemical evolution is due to the death of massive stars. In the other case the progenitors are also massive stars, leading to two supernova explosions in a binary system, which – if not disrupted – causes a binary neutron star system and a merger with a

given delay time due to gravitational radiation losses. Thus, one needs to consider two aspects: (i) the two supernova explosions and the pollution of the ISM with their ejecta (for the case of NS-BH mergers see the discussion in section 5), and (ii) the delay time of the merger event after the formation of the binary neutron star system. Especially aspect (i) can only be treated adequately with inhomogeneous evolution models, and there an additional factor is of major importance: with how much matter the supernova ejecta mix before the neutron star mergers eject their products into the same environment.

This paper is organized as follows. In section 2, we introduce the model used to compute the evolution of abundances. In section 3, we present the influence of the different r- and non-r-process sites on the evolution. Additionally, we provide an overview why an inhomogeneous treatment of the evolution is important. In section 4 we discuss the impact of inhomogeneities, causing and permitting a scatter of $[X/Fe]$ ratios at low metallicities. As a further test of the model, we discuss the fact why the large scatter of $[r/Fe]$ observed at low metallicities is strongly reduced for α -elements, and show how this constraints core collapse supernovae nucleosynthesis predictions, which are still not available in a self-consistent way. In section 5, our results are summarized and discussed.

2 THE MODEL

Recent chemodynamical galactic evolution models, like e.g., Minchev et al. (2014), van de Voort et al. (2015), and Shen et al. (2015), can model in a self-consistent way massive mergers of galactic subsystems (causing effects like infall in simpler models), energy feedback from stellar explosions (causing effects like outflows), radial migrations in disk galaxies, mixing and diffusion of matter/ISM, and the initiation of star formation dependent on local conditions, resulting from the effects discussed above. In our present investigation we still utilize a more classical approach with a parametrized infall of primordial matter, and a Schmidt law (Schmidt 1959) for star formation. Therefore, we neglect large scale mixing effects, while we include the feedback from stellar explosions and the resulting mixing with the surrounding ISM, according to a Sedov-Taylor blast wave. In this way, the model permits to keep track of the local inhomogeneities due to different CCSN ejecta. This approach allows to grasp the main features of the impact of the first stars / stellar deaths on the evolution of the heavy element enrichment. This approximation omits other mixing effects, e.g., spiral arm mixing (on time scales of the order of $2 \cdot 10^8$ years). The main focus of this work is the investigation of the chemical evolution behaviour at low metallicities, where these effects should not have occurred, yet, and are therefore left out in this first order approximation.

We treat the galactic chemical evolution of europium (Eu), iron (Fe) and α -elements (e.g., oxygen O), utilizing the established GCE code "Inhomogeneous Chemical Evolution" (ICE), created by Argast et al. (2004). A detailed description of the model can be found therein.

For the simulation, we set up a cube of $(2kpc)^3$ within the galaxy which is cut in 40^3 smaller cubes representing a $(50pc)^3$ sub cube each. The evolution is followed with time-

M_{tot}	Total infall mass	$10^8 M_{\odot}$
τ	time scale of infall decline	$5 \cdot 10^9$ yrs
t_{max}	time of the highest infall rate	$2 \cdot 10^9$ yrs
t_{final}	duration of the simulation	$13.6 \cdot 10^9$ yrs

Table 1. Main infall parameters. See Argast et al. (2004) for details on the parameters.

steps of 1My. Primordial matter is assumed to fall into the simulation volume, obeying the form

$$\dot{M}(t) = a \cdot t^b \cdot e^{-t/\tau}, \quad (1)$$

which permits an initially rising and eventually exponentially declining infall rate. While τ and the total galaxy evolution time t_{final} are fixed initially, the parameters a and b can be determined alternatively from M_{tot} (the total infall mass integrated over time), defined by

$$M_{tot} := \int_0^{t_{final}} a \cdot t^b \cdot e^{-t/\tau}, \quad (2)$$

and the time of maximal infall t_{max} , given by

$$t_{max} := b \cdot \tau. \quad (3)$$

See Argast et al. (2004) for an extended discussion of the infall model and table 1 for the applied parameters.

2.1 Treating stellar births and deaths

The main calculation loop at each time step (1My) can be described in the following way.

(i) We scan all mass cells of the total volume and calculate the star formation rate per volume and time step (10^6 yrs) according to a Schmidt law with a density power $\alpha = 1.5$ (see Schmidt 1959, Kennicutt 1998, Larson 1991). Dividing by the average stellar mass of a Salpeter IMF (power -2.35) provides the total number of stars per time step $n(t)$ created in the overall volume of our simulation.

(ii) Individual cells in which stars are formed are selected randomly until $n(t)$ is attained, but the probability is scaled with the density, which leads to the fact that patches of higher density, predominantly close to supernova remnants, are chosen.

(iii) The mass of a newly created star is chosen randomly in the range 0.1 to $50M_{\odot}$, subject to the condition that the mass distribution of all stars follows a Salpeter IMF. Consequently only cells which contain more than $50M_{\odot}$ are selected in order to prevent a bias.

(iv) The newly born star inherits the composition of the ISM out of which it is formed.

(v) The age of each star is monitored, in order to determine the end of its lifetime, either to form a white dwarf or experience a supernova explosion (see 2.2.1 and 2.2.2). A fraction of all high mass stars ($M > 8M_{\odot}$), according to the probability (P_{Jet-SN}), is chosen to undergo a magnetorotationally driven supernova event (see section 3.2). Type Ia supernova events are chosen from white dwarfs according to the discussion in 2.2.3. The treatment of neutron star mergers follows the description in 2.2.4.

(vi) The composition for the ejecta of all these events is chosen according to the discussion in 2.2. They will

pollute the neighbouring ISM with their nucleosynthesis products and sweep up the material in a chemically well mixed shell. We assume that an event pollutes typically $5 \cdot 10^4 M_{\odot}$ of surrounding ISM due to a Sedov-Taylor blast-wave of 10^{51} erg (Ryan, Norris & Beers 1996, Shigeyama & Tsujimoto 1998). This implies that the radius of a remnant depends strongly on the local density and the density of the surrounding cells.

(vii) In the affected surrounding cells, stars are polluted by the matter of the previously exploded star and the event specific element yields.

The details on the above procedure will be explained in the following.

2.2 Nucleosynthesis sites

2.2.1 Low (LMS) and intermediate mass stars (IMS)

Low and intermediate mass stars provide a fundamental contribution to the GCE of e.g., He, C, N, F, Na and heavy s-process elements during the asymptotic giant branch (AGB) phase. For instance, most of the C and N in the solar system were made by AGB stars (e.g., Kobayashi 2012). In their hydrostatic burning phase, these stars lock-up a part of the overall mass and return most of it to the ISM in their AGB phase by stellar winds. Since the maximum radius of these winds is orders of magnitude smaller than the output range of supernova events (e.g., radius of Crab remnant: 5.5 Ly (Hester 2008), while the diameter of the Cat’s Eye Nebula is only 0.2 Ly (Reed et al. 1999)), our simulation assumes that stellar winds influence the ISM only in the local calculation cell. AGB stars provide only a marginal s-process contribution to typical r-process elements like Eu (e.g., Travaglio et al. 1999). In particular, for this work the s-process contribution to Eu plays a negligible role and we are not considering it here.

2.2.2 High mass stars (HMS)

Massive stars which exceed $8M_{\odot}$ are considered to end their life in a core-collapse supernova (CCSN, e.g., Thielemann et al. 1996, Nomoto et al. 1997, Woosley et al. 2002, Nomoto et al. 2013, Jones et al. 2013). CCSNe produce most of the O and Mg in the chemical inventory of the galaxy. They provide an important contribution to other α -elements (S, Ca, Ti), to all intermediate-mass elements, the iron-group elements and to the s-process species up to the Sr neutron-magic peak (e.g., Rauscher et al. 2002). Associated to CCSNe, different neutrino-driven nucleosynthesis components might be ejected and contribute to the GCE (e.g., Arcones & Thielemann 2013, and references therein), possibly including the r-process. We did not include regular CCSNe as a major source of heavy r-process elements, as recent investigations indicate strongly that the early hopes for a high entropy neutrino wind with the right properties (Woosley et al. 1994, Takahashi et al. 1994) did not survive advanced core collapse simulations (e.g., Liebendörfer et al. 2003) which led to proton-rich environments in the innermost ejecta (see also Fischer et al. 2010, Hüddepohl et al. 2010), causing rather a so-called νp -process (Fröhlich et al. 2006a, Fröhlich et al. 2006b, Pruet et al.

2005, Pruet et al. 2006, Wanajo 2006). Further investigations seem to underline this conclusion (recently revisited by Wanajo 2013), although a more advanced – in medium – treatment of neutrons and protons in high density matter causes possible changes of the electron fraction (Y_e) of ejecta (Martinez-Pinedo et al. 2012; Roberts et al. 2012) and might permit a weak r-process, including small fractions of Eu. Similar effects might be possible via neutrino oscillations (Wu et al. 2014). For this reason we did not include regular CCSNe in our GCE simulations, although a weak r-process with small (Honda et al. 2006-like) Eu contributions could be responsible for a lower bound of [Eu/Fe] observations (see Fig. 5), explaining a non-detection of the lowest predicted [Eu/Fe] ratios. Nucleosynthesis yields for HMS are taken from Thielemann et al. (1996) or Nomoto et al. (1997). Assuming a typical explosion energy of 10^{51} erg, the ejecta are mixed with the surrounding interstellar medium via the expansion of a Sedov-Taylor blast wave, which stops at a radius which contains about $5 \cdot 10^4 M_{\odot}$ (see section 2.1 for details on the iteration procedure).

2.2.3 Supernovae Type Ia (SNIa)

When an IMS is newly born in a binary system, there is a probability that it has a companion in the appropriate mass range leading finally to a SNIa, following a double- or single degenerate scenario. We follow the analytical suggestion of Greggio (2005) and reduce the numerous degeneracy parameters to one probability ($P_{SNIa} = 9 \cdot 10^{-4}$) for a newly born IMS to actually be born in a system fulfilling the prerequisites for a SNIa. Once the star enters its red giant phase, we let the system perform a SNIa-type explosion and emit the event specific yields (cf. Iwamoto et al. 1999, model CDD2), which highly enriches the surrounding ISM with iron. For this work we use the same SNIa yields for each metallicity, consistently with the Argast et al. (2004) calculations. We are aware that this choice is not optimal, since several SNIa yields including e.g., Mn and Fe depend on the metallicity of the SNIa progenitor (e.g., Timmes et al. 2003, Thielemann et al. 2004, Travaglio et al. 2005, Bravo et al. 2010, Seitenzahl et al. 2013). On the other hand, this approximation does not have any impact on our analysis and our conclusions.

2.2.4 Neutron Star Merger (NSM)

If two newly born HMS were created in a binary system, they may both undergo a CCSN individually. This could leave two gravitationally bound Neutron Stars (“NS”) behind. Such a system emits gravitational waves and the two NS spiral inwards towards their common center of mass with a coalescence time (t_{coal}) until they merge. The actual merging event is accompanied by an ejection of matter and (r-process) nucleosynthesis (Rosswog 2013, Freiburghaus et al. 1999, Panov et al. 2008, Korobkin et al. 2012, Bauswein et al. 2013, Rosswog 2013, Rosswog et al. 2014, Eichler et al. 2014, Wanajo et al. 2014). As all of these publications show the emergence of a strong r-process, in the mass region of Eu they suffer partially from nuclear uncertainties related to fission fragment distributions (see e.g., Eichler et al. 2014, Goriely et al. 2013). For our purposes we chose to utilize as total amount of r-process ejecta

$1.28 \cdot 10^{-2} M_{\odot}$ (consistent with the $1.4 M_{\odot} + 1.4 M_{\odot}$ NS collision in Korobkin et al. 2012 and Rosswog 2013), but distributed in solar r-process proportions, which leads for Eu to a total amount of $10^{-4} M_{\odot}$ per merger. This value is relatively high in comparison to other investigations in the literature.

Observational constraints for the probability of a newly born star to undergo this procedure (P_{NSM}) are provided by e.g., Kalogera et al. (2004) who have found a NSM rate of $R_{NSM} = 83.0_{-66.1}^{+209.1} \text{ Myr}^{-1}$, which corresponds to a $P_{NSM} = 0.0180_{-0.0143}^{+0.0453}$. The coalescence time, P_{NSM} and the event specific yields are important parameters for GCE, and their influence on the GCE are subject of this paper. Concerning the coalescence time scale, it might be more realistic to use a distribution function (e.g., as in Ishimaru, Wanajo & Prantzos 2015) instead of a fixed value. We utilize this simplified procedure as a first order approach.

2.2.5 Magnetorotationally driven supernovae (Jet-SNe)

A fraction (P_{Jet-SN}) of high mass stars end their life as a "magneto-rotationally driven supernova" or magnetar, forming in the center a highly magnetized neutron star (with fields of the order 10^{15} Gauss) and ejecting r-process matter along the poles of the rotation axis (Fujimoto et al. 2006, Fujimoto et al. 2008; Winteler et al. 2012, Mösta et al. 2014). r-process simulations for such events were first undertaken in 3D by Winteler et al. (2012). For the purpose of this work, we randomly choose newly born high mass stars to later form a Jet-SN. At the end of their life time, they explode similar to a CCSN, however with different ejecta. Based on Winteler et al. (2012), we assume an amount of $14 \cdot 10^{-5} M_{\odot}$ of europium ejected to the ISM by such an event. In this work, we study the influence of P_{Jet-SN} and the specific Jet-SN yields on the GCE.

2.3 Observed stellar abundances

Data for the observed stars to compare our simulation results with are taken from the SAGA (Stellar Abundances for Galactic Archaeology) database (e.g., Suda et al. 2008, Suda et al. 2011, Yamada et al. 2013; in particular [Eu/Fe] abundance observations are mainly from e.g., Francois et al. 2007, Simmerer et al. 2004, Barklem et al. 2005, Ren et al. 2012, Roederer et al. 2010, Roederer et al. 2014a, Roederer et al. 2014b, Roederer et al. 2014c, Shetrone, Côté, Stetson 2001, Shetrone et al. 2003, Geisler et al. 2005, Cohen & Huang 2009, Letarte et al. 2010, Starkenburg et al. 2013, McWilliam et al. 2003). From the raw data, we excluded carbon enriched metal poor stars ("CEMPs") and stars with binary nature, since the surface abundances of such objects are expected to be affected by internal pollution from deeper layers or pollution from the binary companion.

3 RESULTS

For a general understanding of the effects of Jet-SNe and NSM on GCE, namely the parameters P_{NSM} , t_{coal} and P_{Jet-SN} , we performed a number of simulations described in detail below.

3.1 Coalescence time scale and NSM probability

As a prerequisite, we studied the influence of both coalescence time and the probability of a binary system to become a NSM. In Figure 1, we present the evolution of [Eu/Fe] abundances when only NSM contribute to the enrichment. The results can be summarized as follows.

(i) Smaller coalescence time scale leads to an enrichment of europium at lower metallicities. Larger coalescence time scale shifts this to higher metallicities.

(ii) A higher NSM probability shifts towards a quantitatively higher enrichment combined with an appearance at lower metallicities.

These effects can be explained in the following way.

(i) When binary neutron star systems take longer to coalesce, the time between the CCSN of both stars and the NSM event is longer. The longer this delay time, also further nucleosynthesis events occur in the galaxy during this period, enriching the ISM with metals. Thus, when the NSM event finally takes place, surrounding stars have developed a higher [Fe/H] abundance, shifting the system towards higher [Eu/Fe] abundances, respectively. This implies an overall europium production shift towards higher metallicities.

(ii) With more binary systems becoming NSM, the produced europium amount per time step is larger, since every event produces the same amount of r-process elements. This leads to a higher [Eu/Fe] abundance, compared to simulations with lower NSM probability. As the fraction of NSM systems is higher while the CCSN rate is constant, larger amounts of europium are produced, while the surrounding medium evolves regularly. This also leads to a higher abundance of europium at lower [Fe/H]. These effects shift the [Eu/Fe] curve to higher values for the same [Fe/H].

All these results are consistent with the earlier conclusions by Argast et al. (2004), stating that it is extremely difficult to reproduce the observed [Eu/Fe] ratios at metallicities $[\text{Fe}/\text{H}] < -2.5$ by NSM alone. A potential solution would be that the preceding supernovae which produced the two neutron stars of the merging system mix their ejecta with more extended amounts of the ISM. We utilized the results following a Sedov-Taylor blast wave of 10^{51} erg, which pollutes of the order $5 \cdot 10^4 M_{\odot}$ of ISM until the shock is stopped. van de Voort et al. (2015) assumed (in their standard case) the mixing with more than $10^6 M_{\odot}$ of ISM (Shen et al. 2015 utilized $2 \cdot 10^5 M_{\odot}$ in a similar approach). This produces an environment with a substantially lower [Fe/H] into which the NSM ejecta enter. Thus, it is not surprising that in such a case the Eu enrichment by NSM is setting in at lower metallicities. The higher resolution run shown in Fig. 4 of van de Voort et al. (2015) agrees with our results. Thus, the major question is whether such a very much enlarged mixing with the ISM by almost two orders of magnitude can be substantiated. We will discuss these aspect further in section 5

3.2 Probability of Jet-SNe

The contribution of Jet-SNe to the galactic Eu abundance differs from that of NSM. Since Jet-SNe explode directly from a massive star, they contribute much earlier to the

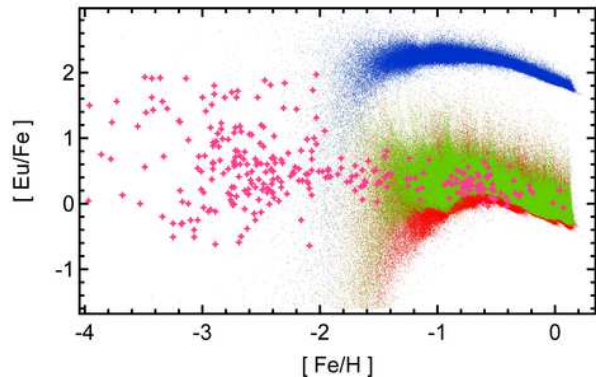


Figure 1. Influence of coalescence time scale and NSM-probability on Eu-Abundances in GCE. Magenta stars represent observations. Red dots correspond to model star abundances as in Argast et al. (2004). The coalescence time scale of this event is 10^8 years and the probability P_{NSM} is set to $4 \cdot 10^{-4}$. Green dots illustrate the effect on the abundances if the coalescence time scale of NSM is shorter (around 10^6 years). Blue dots show the abundance change if the probability of HMS binaries to later merge in a NSM is increased to $4 \cdot 10^{-2}$ (cf. subsection 3.1).

chemical evolution than NSM. Since the interstellar matter is distributed more inhomogeneously than in later evolution stages of the galaxy, high $[\text{Eu}/\text{Fe}]$ abundances are possible in individual stars. This leads to a large spread in the abundances towards lower metallicities. Considering Jet-SNe, the parameter with the highest impact on GCE for such rare events, similar to NSM events but "earlier" in metallicity, is the probability of a massive star to actually become a Jet-SN. A lower probability leads to a smaller overall $[\text{Eu}/\text{Fe}]$ abundance, while a higher probability leads to larger abundances. However, we also recognize a larger spread in abundances in models with lower probability. This comes from the fact that the high yield of the event only sets an upper limit on the abundances. The rarer an event is, the more and the longer stars remain unpolluted. This results in a larger spectrum of abundances in stars and therefore in a larger spread in $[\text{Eu}/\text{Fe}]$ ratios. Note from Fig. 2 and Fig. 3 that Jet-SNe might explain the abundances at low metallicities better than NSM. Thus, while Jet-SNe alone could be an explanation for the lower metallicity observations, there is clear evidence of NSM events and therefore we have to examine the combination of both events. Whether the apparently high concentration of model stars with low $[\text{Eu}/\text{Fe}]$ values at metallicities $-3 < [\text{Fe}/\text{H}] < 2$ in comparison to observations is related to observational bias or whether we require another additional source will be discussed in the following sections.

3.3 Combination of sites

If both sites (Jet-SN and NSM) are considered to contribute to the galactic europium abundances, their contributions overlap. Therefore, parameters which lead to the observed $[\text{Eu}/\text{Fe}]$ abundances, have to be searched for. As described in section 3.1, NSM contribute at a delayed stage to the GCE and in our simulations are unable to reproduce europium abundances at metallicities $[\text{Fe}/\text{H}] < -2.5$, Jet-SNe, however, contribute europium early, but only in those re-

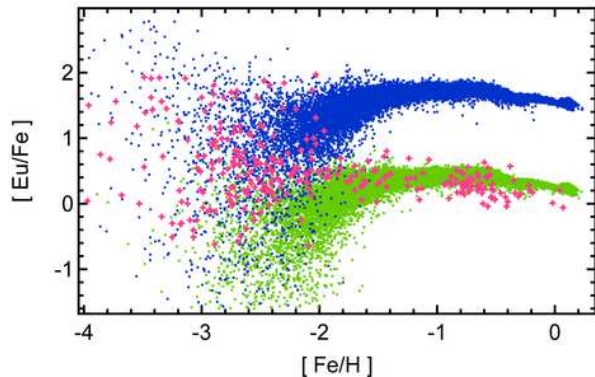


Figure 2. Influence of increased Jet-SN probabilities on Eu-Abundances in GCE. Magenta stars represent observations. Green dots represent model star abundances based on Winteler et al. (2012), the Jet-SN probability has been chosen to follow the observations at $[\text{Fe}/\text{H}] > -1.5$. A good value seems to be 0.1% of HMS to end up in a Jet-SN. Note that this model fails to reproduce the observed abundances at lower metallicities. Blue dots illustrate the effect on the abundances if the Jet-SN probability is increased to 1%. This model better reproduces the observed abundances at lower metallicities, but clearly fails at higher ones.

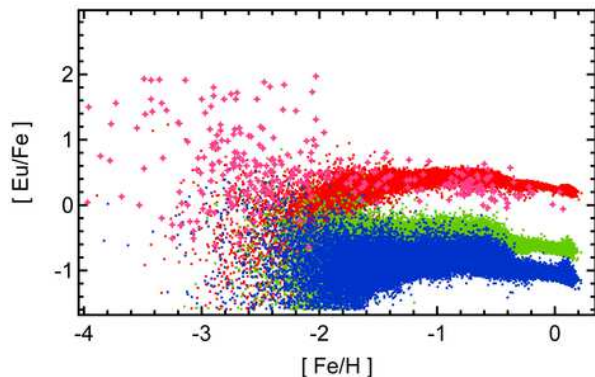


Figure 3. Same as Figure 2, but with decreased probabilities. Red dots are the same as green dots in Fig. 2 with Jet-SN probability of 0.1%; Green and blue dots represent a Jet-SN probability of 10^{-4} and $2 \cdot 10^{-5}$, respectively. From the comparison of these models, we can see how decreased event probability shifts the abundance curve down. We also remark an increase of the spread in abundances when the probability is lowered. The rarer a high yield event is, the larger is the spread in abundances.

gions where they occurred, and cause a larger spread in the $[\text{Eu}/\text{Fe}]$ values (cf. section 3.2). We have to test whether it is possible to use the same parameters as in sections 3.1 and 3.2, since the full combination of both events could lead to an overproduction of elements. We can use the earlier parameter explorations to tune the simulated abundance pattern in order to match the observations. In the following, we will discuss two possible cases:

- (i) $P_{NSM} = 3.4 \cdot 10^{-4}$, $P_{Jet-SN} = 0.3\%$, $t_{coal} = 1\text{My}$ (hereafter model Jet+NSM:A). The results for the model Jet+NSM:A in comparison with observations are shown in Figure 4. This model provide a reasonable explanation of the observations at lower and higher metallicities, but there is an overproduction of europium between $-2 < [\text{Fe}/\text{H}] <$

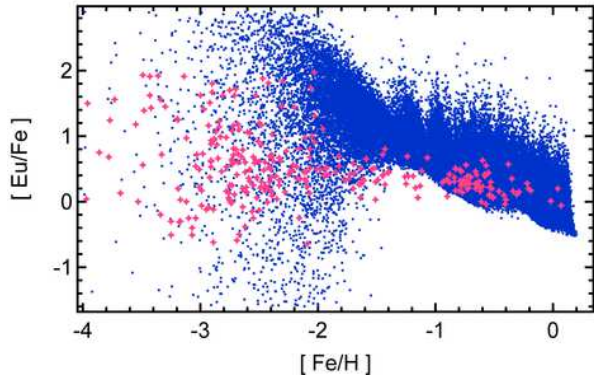


Figure 4. Evolution of Eu-abundances in GCE including both Jet-SNe and NSM as r-process sites. Magenta stars represent observations, whereas blue dots represent model stars. Model (Jet+NSM:A) parameters are $P_{NSM} = 3.4 \cdot 10^{-4}$, $P_{Jet-SN} = 0.3\%$, $t_{coal} = 1\text{My}$.

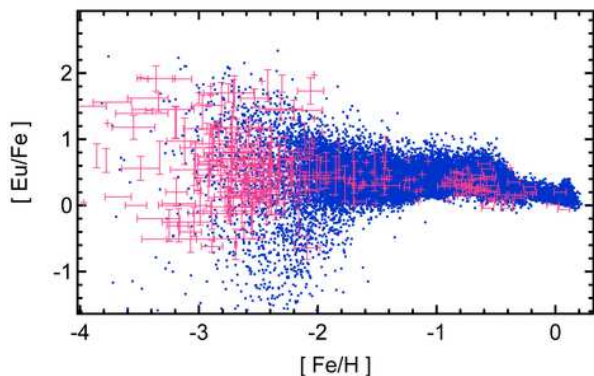


Figure 5. Same as Figure 4, but with a different parameter set (Model Jet+NSM:B). Magenta stars represent observations (with observational errors; however, magenta stars at low metallicities which carry only horizontal errors represent upper limits). Blue dots represent model stars with $P_{NSM} = 3.8 \cdot 10^{-4}$, $P_{Jet-SN} = 0.1\%$, $t_{coal} = 10\text{My}$.

-1. We conclude that larger coalescence time scales and larger probabilities are necessary regarding NSM, and lower probability of Jet-SNe is necessary to flatten and lower the modelled abundance curve.

(ii) $P_{NSM} = 3.8 \cdot 10^{-4}$, $P_{Jet-SN} = 0.1\%$, $t_{coal} = 10\text{My}$ (Model Jet+NSM:B). The results for the model Jet+NSM:B in comparison with observations are shown in Figure 5. This model explains the main features of the abundance curve quite well: The spread at low metallicities, the first confinement of the spread at $[\text{Fe}/\text{H}] \approx -2$, the plateau between $[\text{Fe}/\text{H}] \approx -2$ and $[\text{Fe}/\text{H}] \approx -0.6$, and the second confinement of the spread at $[\text{Fe}/\text{H}] \approx -0.2$. However, there still seem to be difficulties at $[\text{Fe}/\text{H}] \approx -2$: the scatter in abundances towards low $[\text{Fe}/\text{H}]$ ratios seems to be a bit too broad. This spread might be slightly reduced by additional mixing terms (e.g., spiral arms mixing) or an additional source providing ratios of $[\text{Eu}/\text{Fe}] = -1$, which we did not consider in this work.

Considering Fig. 4 and Fig. 5: While the results from both models Jet+NSM:A and Jet+NSM:B can reproduce

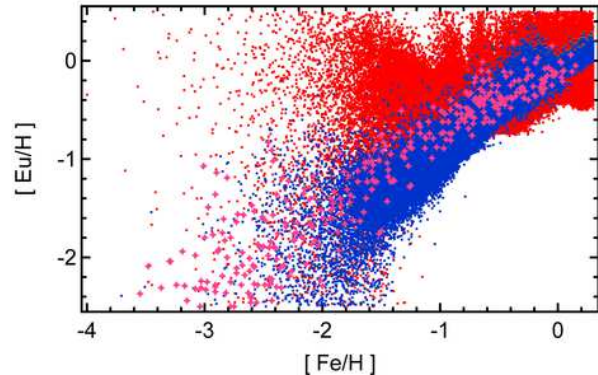


Figure 6. Enrichment history for models Jet+NSM:A and Jet+NSM:B (cf. Figure 4 and 5 for evolution plots). Magenta stars represent observations, whereas blue dots represent model stars as per Figure 5 (Model Jet+NSM:B). Red dots representing the enrichment history of the simulation as per Figure 4 (Model Jet+NSM:A) do not suit the observational data.

the observed spread of $[\text{Eu}/\text{Fe}]$ in the early galaxy, model Jet+NSM:B seems to better fit the overall $[\text{Eu}/\text{Fe}]$ vs. $[\text{Fe}/\text{H}]$ distribution. On the other hand, the evolution of the $[\text{Eu}/\text{Fe}]$ ratio at low metallicity depends on the r-process production and on the Fe production in CCSNe (see Section 4 and discussion). In Fig. 6, we compare the results for the enrichment history of europium in the galaxy according to Jet+NSM:A and Jet+NSM:B models with observations. While the $[\text{Eu}/\text{H}]$ vs. $[\text{Fe}/\text{H}]$ ratios predicted by model Jet+NSM:B are in agreement with the observations, model Jet+NSM:A seems to be ruled out.

4 THE IMPORTANCE OF INHOMOGENEITIES

4.1 Inhomogeneities in GCE

From observations of $[\text{Eu}/\text{Fe}]$ in the early galaxy, one of the main features is a spread in the abundance ratios. Our model is able to reproduce these spreads, mainly because of the inhomogeneous pollution of matter. In Fig. 7, we try to illustrate the effect of applying such an inhomogeneous model. For this purpose, we perform a cut through the xy-plane of the simulation volume for specific time steps. These time steps are marked in the top panel of Fig. 7, in order to provide the reader with a quick glance of the extent of the inhomogeneous element distribution at the correspondent metallicities. For each marker, we provide the complete density field at this specific time step in the middle and lower panels (cf. figure caption for details). We show the extent of inhomogeneities in the middle left panel, for the first marker in the upper panel of the Figure. At this time step, we can see - by counting the "bubble"-style patterns - that at least three supernovae must have taken place before the snapshot. Since such events give rise to nucleosynthesis, the abundances of metals in such a supernova remnant bubble are higher than outside such a remnant. A star being born *inside* such a remnant will inherit more metals than a star born *outside*. Therefore, in the early stages of galactic evolution the stellar abundances are strongly affected by

the location *where* a star is born. Considering much later stages of the evolution, (e.g., the lower right panel of Fig. 7, corresponding to the fourth marker of the upper panel) the supernova remnants have a large overlap. Numerous supernova explosions, have contributed lots of nucleosynthesis all over the galaxy. This leads to an averaged distribution of abundances, including different events and an integral over the initial mass function of stars. Therefore, it resembles a "mixed" phase of galactic evolution, where the elements have been homogenised over the whole volume. At this stage of the evolution, it seems not to be so relevant *where* a star was born. As a consequence, there are smaller differences in the abundance of metals in stars. Therefore, a *confinement* in the spread of abundances of chemical elements at later stages of the chemical evolution is obtained. Becoming more and more homogeneous, the $[\text{Eu}/\text{Fe}]$ value converges to a value that can be obtained by integrating the event yields over the whole IMF.

4.2 Instantaneous Mixing Approximation

A number of recent chemical evolution studies revoked the "instantaneous mixing approximation" (I.M.A., e.g., Chiappini et al. 2001, Recchi et al. 2001, Spitoni et al. 2009). The I.M.A. simplifies a chemical evolution model in terms of mass movement. In detail, all event outputs are expected to mix with the surrounding ISM instantaneously. Such approaches always result in an average value of element ratios for each $[\text{Fe}/\text{H}]$. Therefore, the I.M.A. scheme all stars at a given time inherit the same abundance patterns of elements and it is impossible to reproduce a scatter in the galactic abundances, which seems to be a crucial ingredient at low metallicities. Indeed, instead of a spread of distributions only one value is obtained for each metallicity. We calculate the best fit model (Jet+NSM:B, cf. Fig. 5) with I.M.A. The result can be found in Fig. 8. The I.M.A. approach may be used to study the chemical evolution trends with a lower computational effort, but Figure 7 shows that the reproduction of spreads in abundance ratios due to local inhomogeneities requires to use more complex codes as e.g., the ICE code adopted for this work.

While inhomogeneous GCE codes can explain the spread in r-process elements, there is the question whether they might predict a far too large spread for other elements (e.g., α elements) at low metallicities (with present stellar yields from artificially induced CCSN explosion models). Such effects can also be seen in Fig. 1 in van de Voort et al. (2015) for $[\text{Mg}/\text{Fe}]$, spreading by more than 1 dex, while observations seem to show a smaller spread up to 0.5 dex. This can be related to the amount of supernova ejecta being mixed with the ISM (see discussion above and in section 5: a more extended mixing reduces this spread), but it can also be related to the supernova nucleosynthesis yields which were never tested before in such inhomogeneous GCE studies. From general considerations of chemical evolution studies, it is found that there are large uncertainties for GCE studies, particularly the influence of stellar yields (e.g., Romano et al. (2010)). In Fig. 9, we show the results of model Jet+NSM:B, using the CCSN yields from from Nomoto et al. (1997) and Nomoto et al. (2006), which confirms a large spread in $[\text{O}/\text{Fe}]$, similar to van de Voort et al. (2015) for $[\text{Mg}/\text{Fe}]$. However, present supernova yields are

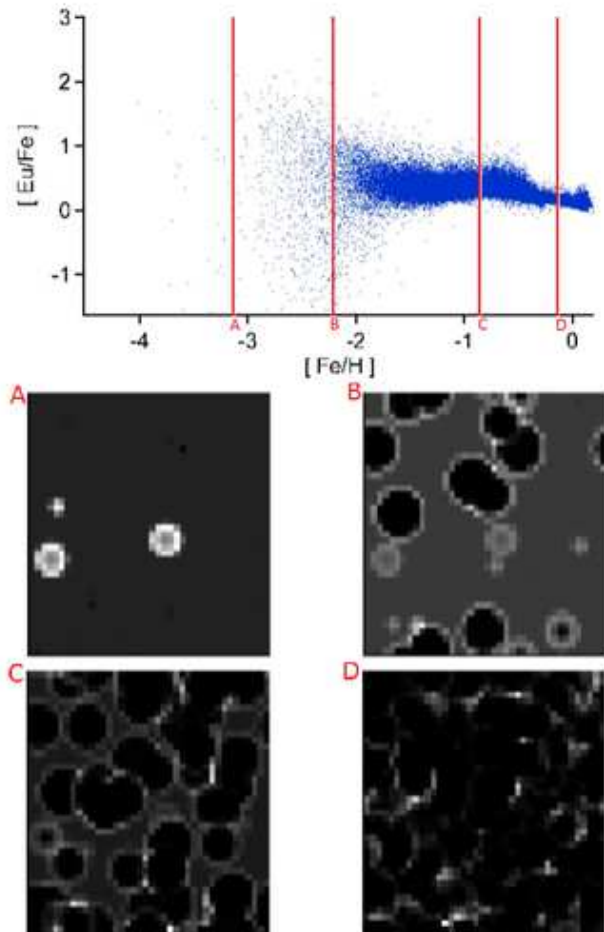


Figure 7. The top panel shows the same GCE-model as in Fig. 5 (Model Jet+NSM:B), but without observations; The red markers refer to the position where a density determination cut through the the xy-plane of the simulation volume is performed. The middle and lower two panels show the density distribution through these planes. The middle left panel corresponds to the very left marker "A" position's density profile (approximately 180 million years (My) have passed in the simulation), the middle right panel to the second marker "B" (≈ 290 My), the lower left panel to the third marker "C" (≈ 2 Gy) and the lower right panel to the very right marker "D" (≈ 12 Gy).

the result of artificially induced explosions with constant explosion energies of the order of 10^{51} erg. If we consider that explosion energies might increase with the compactness of the stellar core (i.e., progenitor mass, e.g., Perego et al. 2015), the heavier α -elements and Fe might be enhanced as a function of progenitor mass. On the other hand O, Ne, and Mg yields are dominated by hydrostatic burning and also increase with progenitor mass (e.g., Thielemann et al. 1996). This could permit to obtain more constant α/Fe ratios over a wide mass range, although the total amount of ejecta differs (increases) as a function of progenitor mass. This scenario does not take into account all the complexity and the multi-dimensional nature of the CCSN event (e.g., Hix et al. 2014, and references therein) that should be considered, but it may be interesting to test its impact in our GCE simulations. In Figs. 9 and 10, we show the results for tests where we:

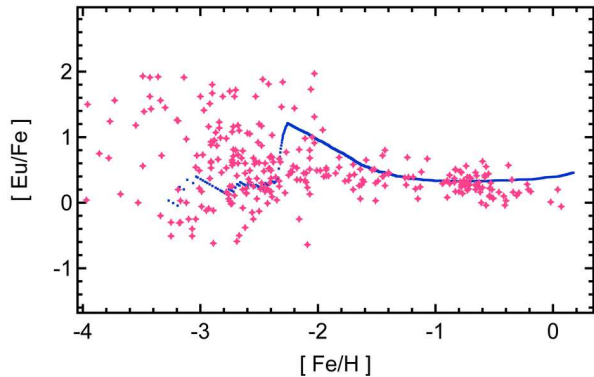


Figure 8. Same GCE-model as in Fig. 5 (Model Jet+NSM:B); however I.M.A. is applied instead of inhomogeneous evolution. One is able to observe a trend in the abundance evolution, however the scatter in the abundance pattern is not present anymore (cf. Section 4 for further discussion). The kink at about $[\text{Fe}/\text{H}] = -2.5$ is related to the delayed time when NSMs set in and contribute to Eu as well. This Figure can also be compared to Fig. 2 in Matteucci et al. (2014) which shows the contribution of NSMs alone for various merger delay times and Eu production yields and Fig. 5 in Vangioni et al. (2015) [mergers alone being indicated by black lines]. Thus, also in this approach it is evident that the explanation of $[\text{Eu}/\text{Fe}]$ at low(est) metallicities by NSM alone is not possible.

- (i) replace the Nomoto et al. (1997) iron yields by *ad-hoc* yields, fitting, however, the observed SN1987A iron production;
- (ii) keep the same CCSN rate as in the previous models;
- (iii) adopt the parameters to study the r-process nucleosynthesis of Model Jet+NSM:B, obtaining the same $[\text{Eu}/\text{H}]$ ratio.

This leads, based on the adopted CCSN yields, to a possibility to minimize the spread in α -elements at low metallicities, while keeping the spread in the r-process element evolution. Therefore, the spread of $[\text{O}/\text{Fe}]$ obtained from GCE simulations for the early galaxy is strongly affected by the uncertainties in the stellar yields, and it is difficult to disentangle them from more intrinsic GCE uncertainties. This means that at this stage it is not obvious whether an overestimation of the observed $[\text{O}/\text{Fe}]$ spread is a problem of the ICE code, the observations could rather provide a constraint on stellar yields. In particular, the use of realistic, self-consistent, explosion energies, might reduce the spread at low metallicities to a large extent. Another fundamental point is related to the discussion in Section 3 concerning $[\text{Eu}/\text{Fe}]$. At this stage, we consider $[\text{Eu}/\text{H}]$ as more constraining to study the r-process nucleosynthesis compared to $[\text{Eu}/\text{Fe}]$, since Fe yields from CCSNe are affected by large uncertainties. Therefore, the model Jet+NSM:B is recommended compared to Jet+NSM:A (see also Fig. 6).

5 CONCLUSION AND DISCUSSION

The main goal of this paper was to reproduce the solar europium abundance as well as the evolution of $[\text{Eu}/\text{Fe}]$ vs. $[\text{Fe}/\text{H}]$ throughout the evolution of the galaxy. For this rea-

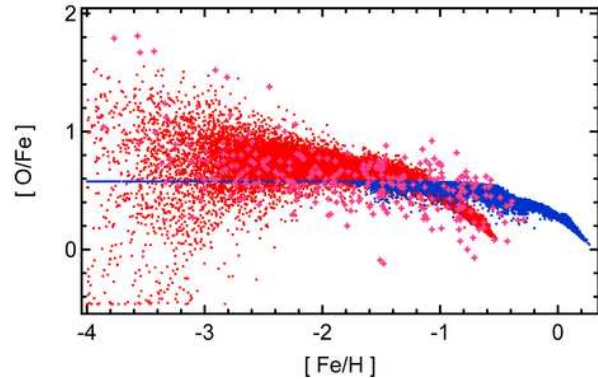


Figure 9. Same GCE-model as in Fig. 5 (Model Jet+NSM:B); Red dots show the abundance evolution of Oxygen when Nomoto et al. (1997) yields are employed, while blue dots represent a far narrower spread at low metallicities if *ad hoc* yields are applied (which still would need to be optimized to obtain a better agreement with the metallicity evolution between $-1 < [\text{Fe}/\text{H}] < 0$). Note that the downturn at high metallicities is shifted to higher $[\text{Fe}/\text{H}]$ values. This is probably due to an overestimate of the total IMF-integrated Fe-production, which should be improved with realistic self-consistent explosion models and their iron yields. While the delay time scale for SNIa is unchanged, earlier CCSN produce more iron, thus dispersing the whole abundance curve. Here we only want to show how changes to possibly more realistic, progenitor-mass dependent, explosion energies can improve the $[\alpha/\text{Fe}]$ spread, while the $[\text{r}/\text{Fe}]$ spread is conserved. (Cf. Section 4 for further discussion.)

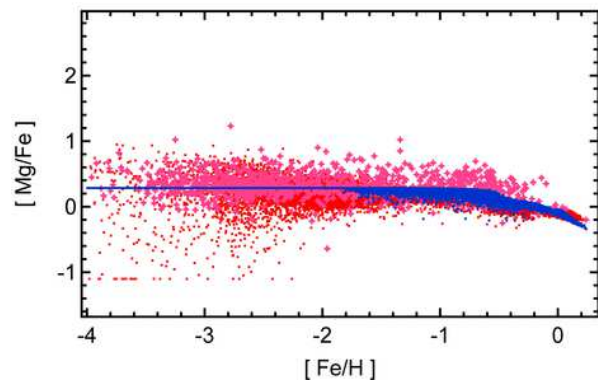


Figure 10. Same consideration as in Fig. 9, however with magnesium instead of oxygen. GCE-model as in Fig. 5 (Model Jet+NSM:B); Red dots show the abundance evolution of magnesium when Thielemann et al. (1996) / Nomoto et al. (1997) yields are employed, while blue dots represent a far narrower spread at low metallicities if *ad hoc* yields are applied. Cf. Section 4 for further discussion.)

son we have studied the influence of two main r-process sites (NSM and Jet-SNe) on the GCE.

Our simulations were based on the inhomogeneous chemical evolution (ICE) model of Argast et al. (2004), with updated nucleosynthesis input for the two sites considered, their respective occurrence frequencies / time delays, and a model resolution of $(50pc)^3$. The main conclusions are that:

- (i) The production of heavy r-process matter in NSM is evident since many years (see Freiburghaus et al. 1999

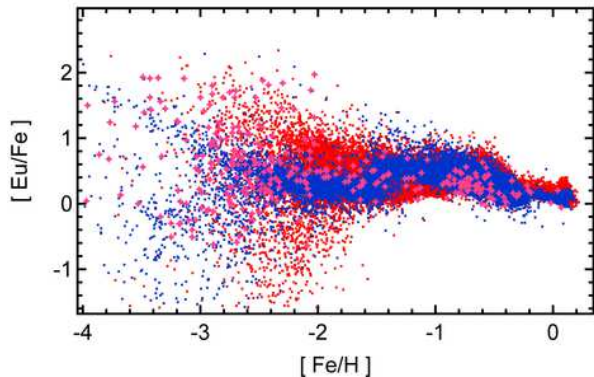


Figure 11. Effect of slightly increased sweep-up mass on GCE. Magenta stars represent observations. Red dots show model stars as per our reference model JET+NSM:B. Blue dots represent a model where every CCSN pollutes $2 \cdot 10^5 M_{\odot}$ of ISM. The dominant effect of this increased sweep up mass is to decrease the scatter of abundances and to shift the abundance curve towards lower metallicities.)

and many later investigations up to Korobkin et al. 2012, Rosswog 2013, Bauswein et al. 2013, Rosswog et al. 2014, Just et al. 2014, Wanajo et al. 2014, Eichler et al. 2014, Mendoza et al. 2015). Our implementation of NSM in the inhomogeneous chemical evolution model "ICE" can explain the bulk of Eu (r-process) contributions in the galaxy for $[\text{Fe}/\text{H}] > -2.5$, but have problems to explain the amount and the spread of $[\text{Eu}/\text{Fe}]$ at lower metallicities. This is in agreement with the initial findings of Argast et al. (2004). Recent SPH-based studies by van de Voort et al. (2015) make use of a mixing of the ejecta with $3 \cdot 10^6 M_{\odot}$, a further study by Shen et al. (2015) utilizes a mixing with $2 \cdot 10^5 M_{\odot}$ up to $8 \cdot 10^5 M_{\odot}$. The mixing volume we utilize, based on the Sedov-Taylor blast wave approach, would be related to a subgrid-resolution in these studies, but this treatment is essential for the outcome. Mixing initially with a larger amount of matter causes smaller $[\text{Fe}/\text{H}]$ ratios into which the r-process material is injected.

We have tested such differences in mixing volumes/masses also within our ICE approach. Fig. 11 shows the results we obtain when changing from the Sedov-Taylor blast wave approach to a mixing mass of $2 \cdot 10^5 M_{\odot}$ (like in Shen et al. 2015), and we can see that we essentially reproduce their results. On the other hand, a higher resolution test in section 3.1 of van de Voort et al. (2015) is essentially in agreement with our results presented above. Thus, these differences are not based on the differences in sophistication of the multi-D hydrodynamics approach, permitting to model energy feedback from supernovae, outflows and infall, they can rather be linked directly to the mixing volumes of supernova ejecta. This requires further studies in order to understand whether there exist physical processes (on the timescale of the delay between the supernova explosions and the merger event) which permit a mixing beyond the Sedov-Taylor blast wave approach.

(ii) The production of heavy r-process elements in a rare species of CCSNe with fast rotation rates and high magnetic fields, causing (fast) jet ejection of neutron-rich matter along the poles has first been postulated by Cameron (2001). This was followed up in rotationally symmetric 2D calcula-

tions Fujimoto et al. (2006), Fujimoto et al. (2008) and the first 3D calculations by Winteler et al. (2012). These calculations still depend on unknown rotation velocities, and magnetic field configurations before collapse, however, they agree with the observations of magnetars and neutron stars with magnetic fields of the order 10^{15} Gauss which make up about 1% of all observed neutron stars. Further 3D calculations by Mösta et al. (2014) and recent 2D calculations by Nishimura et al. (2015), might indicate that not all events leading to such highly magnetized neutron stars are able to eject the heaviest r-process elements in solar proportions. Thus, probably less than 1% of all CCSNe end as Jet-SNe with a full r-process.

When introducing Jet-SNe with ejecta as predicted by Winteler et al. (2012), they can fill in the missing Eu at lower metallicities and reproduce the spread in $[\text{Eu}/\text{Fe}]$, in agreement with the recent findings of Cescutti & Chiappini (2014). We find that a fraction of 0.1% of all CCSNe which end up in this explosion channel provides the best fit. This would mean that not all but only a fraction of magnetar events which produce the highest magnetic field neutron stars are able to eject a main r-process composition of the heaviest elements, as discussed above.

Our conclusion is that both sites acting in combination provide the best scenario for understanding $[\text{Eu}/\text{Fe}]$ observations throughout galactic history, with typical probabilities for NSM formations and (merging) delay times as well as probabilities for Jet-SNe. As a side effect we realized that present supernova nucleosynthesis yield predictions, based on induced explosions with a single explosion energy throughout the whole mass range of progenitor stars, bear a number of uncertainties. While apparently too large scatters of alpha/Fe ratios can be obtained in inhomogeneous chemical evolution models, when utilizing existing nucleosynthesis predictions from artificial explosions with energies of 1 Bethe, this might not be due to the chemical evolution model. Such deficiencies can be cured by assuming larger mixing masses with the ISM for supernovae explosions (van de Voort et al. 2015, Shen et al. 2015), or the introduction of an artificial floor of abundances based on IMF-Integrated yields of CCSNe for metallicities at $[\text{Fe}/\text{H}] = -4$, but it could in fact just be due the non-existence of self-consistent CCSN explosion models. We have shown that an explosion energy dependence on the compactness of the Fe-core, related to the main sequence mass, could solve this problem as well by modifying the nucleosynthesis results. Therefore, self-consistent core collapse calculations with explosion energies varying with progenitor mass and possibly other properties like rotation are highly needed. Although we have obtained a good accordance with the observed Eu abundances, the true origin of r-process elements might still require additional insights. The present investigation may be used to put constraints on the yields, as well as essential properties and occurrence frequencies of sites.

There exist a number of open questions not addressed in the present paper, related (a/b) to production sites and (c) to the true chemical evolution of the galaxy.

(a) As discussed in detail in section 2.2.2, we did not include "regular" CCSNe from massive stars as contributors to the main or strong r-process, producing the heaviest elements in the Universe. However, as already men-

tioned in section 2.2.2, there exists the chance for a weak r-process, producing even Eu in a Honda-style pattern in such events. This could provide the correct lower bound of [Eu/Fe] in Fig. 5 and would be consistent with the recent findings of Tsujimoto & Shigeyama (2014).

(b) We did not include the effect of NS-BH mergers in the present paper. They would result in similar ejecta as NS-NS mergers per event (Korobkin et al. 2012), but their occurrence frequencies bear high uncertainties (Postnov & Yungelson 2014). Mennekens & Vanbeveren (2014) provide a detailed account of their possible contribution and also discuss their contribution to global r-process nucleosynthesis. One major difference with respect to our treatment of NSM in chemical evolution relates to the fact, that (if the black hole formation is not causing a hypernova event but rather occurring without nucleosynthesis ejecta) only one CCSN is polluting the ISM with Fe before the merger event, in comparison to two CCSNe. This would lead to a smaller [Fe/H] ratio in the ISM which experiences the r-process injection, and just to an "earlier" appearance of high [Eu/Fe] ratios in galactic evolution. If we assume that BH formations are as frequent as supernova explosions, an upper limit of the effect would be that all NS-NS mergers are replaced by BH-NS mergers, moving the [Eu/Fe] features to lower metallicities by a factor of 2. However, the lower main sequence mass limit for BH formation is probably of the order $20M_{\odot}$, and only a small fraction of core collapses end in black holes. Therefore, we do not expect that the inclusion of NS-BH mergers shifts the entries by more than 0.15 in Fig. 1. This by itself would not be a solution in terms of making only compact (i.e. NS-NS and NS-BH) mergers responsible for the r-process at very low metallicities.

(c) There have been suggestions that the Milky Way in its present form resulted from merging subsystems with a different distribution of masses. Such "dwarf galaxies" will experience different star formation rates. It is known that different star formation rates can shift the relation [X/Fe] as a function of [Fe/H]. If the merging of such subsystems will be completed at the time when type Ia supernovae start to be important, the relation [X/Fe]=f([Fe/H]) will be uniform at and beyond [Fe/H] > -1, but it can be blurred for low metallicities between the different systems, possibly leading also to a spread of the onset of high [Eu/Fe] ratios at low metallicities (Ishimaru, Wanaajo & Prantzos 2015). The result depends on the treatment of outflows, should in principle be tested in inhomogeneous models, and also already be present in the simulations of van de Voort et al. (2015) and Shen et al. (2015). But it surely requires further investigations to test fully the impact of NSM on the r-process production in the early galaxy.

Future studies will probably require a distribution of delay times for NSM events, a test of the possible contributions by BH-NS mergers, a better understanding of yields, and improvements in understanding mixing processes after supernovae explosions and during galactic evolution. Testing the full set of element abundances from SNe Ia and CCSNe as well as the two sources discussed above, in combination with extended observational data, will provide further clues to understanding the evolution of galaxies.

6 ACKNOWLEDGEMENTS

The authors thank Dominik Argast for providing his GCE code "ICE" for our investigations. MP thanks the support from the Swiss National Science Foundation (SNF) and the "Lendület-2014" Programme of the Hungarian Academy of Sciences (Hungary). BW and FKT are supported by the European Research Council (FP7) under ERC Advanced Grant Agreement No. 321263 - FISH, and the Swiss National Science Foundation (SNF). The Basel group is a member in the COST Action New Compstar. We also thank Almudena Arcones, John Cowan, Gabriel Martínez-Pinedo, Lyudmila Mashonkina, Francesca Matteucci, Tamara Mishenina, Nobuya Nishimura, Igor Panov, Albino Perego, Tsvi Piran, Nikos Prantzos, Stephan Rosswog, and Tomoya Takiwaki for helpful discussions during the Basel Brainstorming workshop; Camilla J. Hansen, Oleg Korobkin, Yuhri Ishimaru, and Shinya Wanaajo for discussions at ECT* in Trento, and Freeke van de Voort for providing details about their modelling. We would also like to acknowledge productive co-operation with our Basel colleagues Kevin Ebinger, Marius Eichler, Roger Käppeli, Matthias Liebendörfer, Thomas Rauscher, and Christian Winteler. Finally, we would also like to thank an anonymous referee who provided useful and constructive suggestions and helped improving the paper.

REFERENCES

- Argast, D., Samland, M., Thielemann, F.-K. and Qian, Y.-Z., 2004 A&A 416, 997–1011
- Arcones, A., Thielemann, F.-K., 2013 JPhG 40 013201 DOI: 10.1088/0954-3899/40/1/013201
- Arlandini, C., Käppeler, F., Wisshak, K., Gallino, R., Lugaro, M., Busso, Ma., Straniero, O., 1999 ApJ 525 886–900, DOI:10.1086/307938
- Audouze, J., Tinsley, B.M., 1976 AR A&A 14 43-79 DOI:10.1146/annurev.aa.14.090176.000355
- Barklem, P. S., et al. 2005, A&A, 439, 129
- Bauswein, A., Goriely, S., Janka, H.-T., 2013 ApJ 773 :78
- Bauswein, A., Pulpillo, R. A., Janka, H. T., Goriely, S., 2014 ApJL 795 (1) L9 DOI:10.1088/2041-8205/795/1/L9
- Bisterzo, S., Travaglio, C., Gallino, R., Wiescher, M., Käppeler, F., 2014 ApJ 787: 10,14, DOI:10.1088/0004-637X/787/1/10
- Bravo, E., Domínguez, I., Badenes, C., Pierantoni, L., Straniero, O., 2010 ApJL 711, L66-L70, DOI:10.1088/2041-8205/711/2/L66
- Cameron, A.G.W., 2001 ApJ 562 456-469 DOI: 10.1086/323869
- Cescutti, G., Chiappini, C., Hirschi, R., Meynet, G., Frischknecht, U., 2013 A&A 553: UNSP A51, DOI: 10.1051/0004-6361/201220809
- Cescutti, G., Chiappini, C., 2014 A& A 565 DOI: 10.1051/0004-6361/201423432
- Chiappini, C., Matteucci, F., Romano, D., 2001 ApJ 554 1044-1058
- Cohen, J. G., Huang, W. 2009 ApJ, 701, 1053
- De Donder, E., Vanbeveren, D., 2003 New Astronomy 8 415-425
- Eichler, M., Arcones, A., Kelic, A., Korobkin, O., Lan- ganke, K., Martinez-Pinedo, G., Panov, I. Rauscher, T.,

- Rosswog, S., Winteler, C., Zinner, N.T., Thielemann, F.-K. 2014 arXiv:1411.0974
- François, P. et al. 2007 *A&A*, 476, 935
- Freiburghaus, C., Rosswog, S., Thielemann, F.-K., 1999 *ApJ* 525 L121
- Fujimoto, S., Hashimoto, M., Kotake, K., Yamada, S., 2006 *Origin of Matter and Evolution of Galaxies* 847, 386-388
- Fujimoto, S., Nishimura, N., Hashimoto, M., 2008 *ApJ* 680 1350-1358 DOI:10.1086/529416
- Fischer, T., Whitehouse, S. C., Mezzacappa, A., Thielemann, F.-K., Liebendörfer, M., 2010 *A&A* 517 A80, DOI:10.1051/0004-6361/200913106
- Fröhlich, C., Martínez-Pinedo, G., Liebendörfer, M., Thielemann, F.-K., Bravo, E., Hix, W., Langanke, K., Zinner, N., 2006 *PRL* 96 14 142502, DOI: 10.1103/PhysRevLett.96.142502
- Fröhlich, C., Hauser, P., Liebendörfer, M., Martínez-Pinedo, G., Thielemann, F.-K., Bravo, E., Zinner, N. T., Hix, W. R., Langanke, K., Mezzacappa, A., Nomoto, K. 2006 *ApJ* 637 415-426, DOI:10.1086/498224
- Geisler, D., Smith, V. V., Wallerstein, G., Gonzalez, G., Charbonnel, C., 2005 *AJ*, 129,1428
- Gibson, B. K., Fenner, Y., Renda, A., Kawata, D., Lee, H., 2003 *Publications of the Astronomical Society of Australia*, 20 4 401-415, DOI: 10.1071/AS03052
- Greggio, L., *A&A* 441, 1055-1078 DOI: 10.1051/0004-6361:20052926
- Goriely, S., Bauswein, A., Janka, H.T., 2012 *Nuclear Physics in Astrophysics V* 337 012039 DOI: 10.1088/1742-6596/337/1/012039
- Goriely, S., Sida, J.-L., Lemaître, J.-F., Panebianco, S., Dubray, N., Hilaire, S., Bauswein, A., Janka, H.-T., (2013) *PRL* 111, 24, DOI:10.1103/PhysRevLett.111.242502
- Goswami, A., Prantzos, N., 2000 *A&A*, 359, 191-212
- Hester, J. J. 2008 *AR A&A* 46 127–155 DOI:10.1146/annurev.astro.45.051806.110608
- Hüdepohl, L., Muller, B., Janka, H.T., Marek, A., Raffelt, G.G., 2010 *PRL* 104 251101 DOI:10.1103/PhysRevLett.104.251101
- Hix, W., Lentz, E., Endeve, E., Baird, M., Chertkow, M., Harris, J., Messer, O. E., Mezzacappa, A., Bruenn, S., Blondin, J., 2014 *AIP Advances* 4 041013, DOI:10.1063/1.4870009
- Honda, S., Aoki, W., Ishimaru, Y., Wanajo, S., Ryan, S. G., 2006 *ApJ* 643 1180
- Ishimaru, Y. & Wanajo, S., 1999 *ApJ* 511 L33-L36 DOI: 10.1086/311829
- Ishimaru, Y., Wanajo, S., Prantzos, N., (2015) *ApJ* 804L 35I, DOI: 10.1088/2041-8205/804/2/L35
- Iwamoto, K., Brachwitz, F., Nomoto, K., et al. 1999, *ApJS* 125 439-462, DOI:10.1086/313278
- Jones, S., Hirschi, R., Nomoto, K., Fischer, T., Timmes, F. X., Herwig, F., Paxton, B., Toki, H., Suzuki, T., Martínez-Pinedo, G., Lam, Y. H., Bertolli, M. G., 2013 *ApJ* 772 2 150
- Just, O. et al. 2014, arXiv1406.2687
- Käppeler, F., Gallino, R., Bisterzo, S., Aoki, W., 2011 *RvMP*, 83 157-194, DOI:10.1103/RevModPhys.83.157
- Kalogera, V., Kim, C., Lorimer, D.R., Burgay, M., D'Amico, N., Possenti, A., Manchester, R.N., Lyne, A.G., Joshi, B.C., McLaughlin, M.A., Kramer, M., Sarkissian, J.M., Camilo, F., 2004 *ApJ* 601 L179-L182
- Kennicutt, R. C. Jr., 1998 *ApJ* 498:541, DOI:10.1086/305588
- Kobayashi, C., Umeda, H., Nomoto, K., Tominaga, N., Ohkubo, T., 2006 *ApJ* 653 1145-1171
- Kobayashi, C., 2012 *AIPC* 1484 90-98, DOI: 10.1063/1.4763379
- Korobkin, O., Rosswog, S., Arcones, A., Winteler, C., *MNRAS* 2012 426 1940-1949. DOI: 10.1111/j.1365-2966.2012.21859.x
- Kouveliotou, C., Dieters, S., Strohmayer, T., et al. 1998, *Nature*, 393, 235
- Kramer, M. 2009, in *IAU Symp. 259, Cosmic Magnetic Fields: From Planets, to Stars and Galaxies*, ed. K. G. Strassmeier, A. G. Kosovichev, & J. E. Beckman (Cambridge: Cambridge Univ. Press), 485
- Kratz, K.-L., Farouqi, K., Mashonkina, L. I., Pfeiffer, B., 2008 *New Astronomy Reviews* 52 390-395, DOI:10.1016/j.newar.2008.06.015
- Larson, R., 1991 *ASPC* 20 571L
- Letarte, B., Hill, V., Tolstoy, E., Jablonka, P., Shetrone, M., et al., 2010 *A&A* 523 A17
- Liebendörfer, M., Mezzacappa, A., Messer, O. E. B., Martínez-Pinedo, G., Hix, W. R., Thielemann, F.-K., 2003 *Nuc Phys A* 719 C144-C152
- Liebendörfer, M., Messer, O.E.B., Mezzacappa, A., Bruenn, S.W., Cardall, C.Y., Thielemann, F.-K., 2004 *ApJ Suppl. Series* 150 263-316 DOI: 10.1086/380191
- Mennekens, N., Vanbeveren, D., (2014) *A&A* 564, A134, DOI:10.1051/0004-6361/201322198
- Martinez-Pinedo, G., Fischer, T., Lohs, A., Huther, L., 2012nuco.confE..54M
- Matteucci, F., *The chemical evolution of the Galaxy, Astrophysics and space science library*, Volume 253, Dordrecht: Kluwer Academic Publishers, ISBN 0-7923-6552-6
- Matteucci, F., 2012 *Chemical Evolution of Galaxies, Astronomy and Astrophysics Library*. ISBN 978-3-642-22490-4. Springer-Verlag Berlin Heidelberg, 2012 DOI: 10.1007/978-3-642-22491-1
- Matteucci, F., Romano, D., Arcones, A., Korobkin, O., Rosswog, S., (2014) *MNRAS* 438 p.2177-2185, DOI:10.1093/mnras/stt2350
- McWilliam, A., Wallerstein, G., Mottini, M. 2013 *ApJ* 778,149
- Mendoza-Temis, J., Martínez-Pinedo, G., Langanke, K., Bauswein, A., & Janka, H.-T., (2014) *ArXiv*
- Minchev, I., Chiappini, C., Martig, M., 2014 *A&A* 572 A92-A92
- Mösta, P., Richers, S., Ott, C.D., Haas, R., Piro, A.L., Boydston, K., Abdikamalov, E., Reisswig, C., Schnetter, E., 2014 *ApJL* 785 L29 DOI: 10.1088/2041-8205/785/2/L29
- Nishimura, N., Takiwaki, T., Thielemann, F.-K., arXiv:1501.06567
- Nomoto, K., Hashimoto, M., Tsujimoto, T., et al. 1997 *Nucl. Phys.A* 616 79c13
- Nomoto, K., Tominaga, N., Umeda, H., Kobayashi, C., Maeda, K., 2006 *Nuc. Phys. A*, 777 424-458 DOI: 10.1016/j.nuclphysa.2006.05.008
- Nomoto, K., Kobayashi, C., Tominaga, N., 2013 *AR A&A* 51 457-509, DOI:10.1146/annurev-astro-082812-140956
- Pagel, B., 2009 *Nucleosynthesis and Chemical Evolution of Galaxies*, Cambridge University Press,

- ISBN:9780521840309 DOI: 10.1017/CBO9780511812170
Panov, I. V.; Korneev, I. Yu.; Thielemann, F.-K., 2008 AL 34 189-197
- Perego, A., Hempel, M., Fröhlich, C., Ebinger, K., Eichler, M., Casanova, J., Liebendörfer, M., Thielemann, F.-K., 2015 arXiv:1501.02845
- Postnov, K. A. & Yungelson, L. R. 2014, Living Rev. Rel., 17, 3
- Pruet, J., Woosley, S. E., Buras, R., Janka, H.-T., Hoffman, R. D. 2005 ApJ 623 325-336 DOI: 10.1086/428281
- Pruet, J., Hoffman, R. D., Woosley, S. E., Janka, H.-T., Buras, R., 2006 ApJ 644 1028-1039. DOI:10.1086/503891
- Qian Y.-Z., 2000 ApJL 534 L67
- Rauscher, T., Heger, A., Hoffman, R. D., Woosley, S. E., (2002) ApJ 576 (1) 323 DOI:10.1086/341728
- Recchi, S., Matteucci, F., D’Ercole, A., 2001 MNRAS 322 800-820, DOI: 10.1046/j.1365-8711.2001.04189.x
- Reed, D. S., Balick, B., Hajian, A. R., Klayton, T. L., Giovanardi, S., Casertano, S., Panagia, N., Terzian, Y., 1999 ApJ 118 2430–2441, arXiv:astro-ph/9907313, doi:10.1086/301091
- Ren, M. et al., 2012 ApJ 755 89
- Roberts, L.F., Kasen, D., Lee, W.H., Ramirez-Ruiz, E., 2011 ApJ 736 L21
- Roederer, I.U. et al., 2010 ApJ 724 975
- Roederer, I.U. et al., 2014 ApJ 784 158
- Roederer, I.U. et al., 2014 AJ, 147 136
- Roederer, I.U. et al., 2014 MNRAS 445 2970
- Romano, D., Karakas, A. I., Tosi, M., Matteucci, F., 2010 A&A 522 A32, 27, DOI:10.1051/0004-6361/201014483
- Stephan Rosswog, 2013 Phil. Trans. R. Soc. A:20120272, DOI: 10.1098/rsta.2012.0272
- Rosswog, S., Korobkin, O., Arcones, A., Thielemann, F.-K., Piran, T., 2014 MNRAS 439 744-756 DOI: 10.1093/mnras/stt2502
- Ryan, S. G., Norris, J. E., and Beers, T. C., 1996 ApJ, 471 254
- Schmidt, M.: 1959 ApJ, 121: 161
- Seitenzahl, I. R., Ciaraldi-Schoolmann, F., Röpke, F. K., Fink, M., Hillebrandt, W., Kromer, M., Pakmor, R., Ruitter, A. J., Sim, S. A., Taubenberger, S., 2013 MNRAS 429 1156-1172, DOI:10.1093/mnras/sts402
- Shen, S., Cooke, R., Ramirez-Ruiz, E., Madau, P., Mayer, L., Guedes, J., Accepted for ApJ 2015 arXiv:1407.3796
- Shetrone, M., Côté, P., Stetson, P. B., 2001 PASP 113 1122
- Shetrone, M., Venn, K. A., Tolstoy, E., Primas, F., Hill, V., Kaufer, A., 2003 AJ125 684
- Shigeyama, T. and Tsujimoto, T., 1998 ApJ 507 L135
- Simmerer, J., et al., 2004 ApJ 617 1091
- Snedden, C., Cowan, J.J., Gallino, R., 2008 AR A&A 46 241
- Spitoni, E., Matteucci, F., Recchi, S., Cescutti, G., Pipino, A., 2009 A&A 504 87-96, DOI: 10.1051/0004-6361/200911768
- Starkenburger, E., Hill, V., Tolstoy, E., Francois, P., Irwin, M. J., Boschman, L., Venn, K. A., de Boer, T. J. L., Lemasle, B., Jablonka, P., Battaglia, G., Groot, P., Kaper, L., 2013 A&A 549 88
- Suda, T., Katsuta, Y., Yamada, S., Suwa, T., Ishizuka, C., Komiya, Y., Sorai, K., Aikawa, M., Fujimoto, M.Y., 2008 PASJ 60 1159-1171
- Suda, T., Yamada, S., Katsuta, Y., Komiya, Y., Ishizuka, C., Aoki, W., Fujimoto, M.Y., 2011 MNRAS 412 843-874
- Takahashi, K., Witt, J., Janka, H.T., 1994 A&A 286 857-869
- Thielemann, F.-K., Nomoto, K., Hashimoto, M., 1996 ApJ 460 408-436
- Thielemann, F.-K., Brachwitz, F., Höflich, P., Martinez-Pinedo, G., Nomoto, K., 2004 New Astronomy Reviews 48 605-610 DOI:10.1016/j.newar.2003.12.038
- Thielemann, F.-K., Arcones, A., Käppeli, R., Liebendörfer, M., Rauscher, T., Winteler, C., Fröhlich, C., Dillmann, I., Fischer, T., Martinez-Pinedo, G., Langanke, K., Farouqi, K., Kratz, K.-L., Panov, I., Korneev, I. K., Progress in Particle and Nuclear Physics 66 346-353, DOI: 10.1016/j.ppnp.2011.01.032
- Timmes, F.X., Woosley, S.E., Weaver, T.A., 1995 ApJ Suppl. Series 98 617-658 DOI: 10.1086/192172
- Timmes, F. X., Brown, E. F., Truran, J. W., 2003 ApJ 590 L83-L86 DOI:10.1086/376721
- Travaglio, C., Galli, D., Gallino, R., Busso, M., Ferrini, F., Staniero, O., 1999 ApJ 521 691-702 DOI: 10.1086/307571
- Travaglio, C., Hillebrandt, W., Reinecke, M., Thielemann, F.-K., 2004 A&A 425.1029T
- Travaglio, C., Hillebrandt, W., Reinecke, M., 2005 A&A, 443 1007-1011 DOI: 10.1051/0004-6361:20052883
- Tsujimoto, T., Shigeyama, T., (2014) A&A 565 id.L5, 4 pp., DOI: 10.1051/0004-6361/201423751
- van den Heuvel, E. P. J., Lorimer, D. R., 1996 MNRAS 283 (2) L37-L40
- van de Voort, F., Quataert, E., Hopkins, P. F., Keres, D., Faucher-Giguère, C.-A., 2015 MNRAS 447 140-148, DOI:10.1093/mnras/stu2404
- Vangioni, E., Goriely, S., Daigne, F., Francois, P., Belczynski, K., arXiv:1501.01115
- Wanajo, S., Sekiguchi, Y., Nishimura, N., Kiuchi, K., Kyutoku, K., Shibata, M., 2014 ApJL 789 L39 DOI: 10.1088/2041-8205/789/2/L39
- Wanajo, S., 2006 ApJ 647 1323W, DOI:10.1086/505483
- Wanajo, S., 2013 ApJL 770 L22 DOI: 10.1088/2041-8205/770/2/L22
- Woosley, S.E., Wilson, J.R., Mathews, G.J., Hoffman, R.D., Meyer, B.S., 1994 ApJ 433 229-246 DOI:10.1086/174638
- Woosley, S. E., Heger, A., Weaver, T. A., 2002 Rev. Mod. Phys., 74 1015-1071 DOI: 10.1103/RevModPhys.74.1015
- Winteler, C., Käppeli, R., Perego, A., Arcones, A., Vassetz, N., Nishimura, N., Liebendörfer, M., Thielemann, F.-K., 2012 ApJ 750 L22
- Wu, M.-R., Qian, Y.-Z., Martinez-Pinedo, G., Fischer, T., Huther, L., 2014 arXiv:1412.8587W
- Yamada, S., Suda, T., Komiya, Y., Aoki, W., Fujimoto, M.Y., 2013 MNRAS 436 1362-1380